Available online at www.sciencedirect.com

SciVerse ScienceDirect

Journal of the European Ceramic Society 33 (2013) 1087–1092

www.elsevier.com/locate/jeurceramsoc

# Sintering of porous alumina obtained by biotemplate fibers for low thermal conductivity applications

Tiago Delbrücke [a], Rogério A. Gouvêa [a], Mário L. Moreira [b], Cristiane W. Raubach [c], José A. Varela [d], Elson Longo [d], Margarete R.F. Gonçalves [a], Sergio Cava [a,*]

[a] Graduate Program in Science and Materials Engineering, Technology Development Center, Federal University of Pelotas, 96010-900 Pelotas, RS, Brazil
[b] Department of Physics, Institute of Physics and Mathematics, Federal University of Pelotas, 96010-900, Pelotas, RS, Brazil
[c] Interdisciplinary Laboratory of Electrochemistry & Ceramics, Federal University of Sao Carlos, 18052-780 São Carlos, SP, Brazil
[d] National Institute of Science and Technology of Materials in Nanotechnology, Paulista State University, 14801-907, Araraquara, SP, Brazil

Received 17 September 2012; received in revised form 7 November 2012; accepted 12 November 2012
Available online 25 December 2012

**Abstract**

In this research report, a sintering process of porous ceramic materials based on $Al_2O_3$ was employed using a method where a cation precursor solution is embedded in an organic fibrous cotton matrix. For porous green bodies, the precursor solution and cotton were annealed at temperatures in the range of 100–1600 °C using scanning electron microscopy (SEM) and thermogravimetric (TG) analysis to obtain a porous body formation and disposal process containing organic fibers and precursor solution. In a structure consisting of open pores and interconnected nanometric grains, despite the low porosity of around 40% (calculated geometrically), nitrogen physisorption determined a specific surface area of 14 $m^2/g$, which shows much sintering of porous bodies. Energy dispersive X-ray (EDX) and X-ray diffraction (XRD) analytical methods revealed a predominant amount of α-$Al_2O_3$ in the sintered samples. Thermal properties of the sintered $Al_2O_3$ fibers were obtained by using the Laser Flash which resulted in the lower thermal conductivity obtained by α-$Al_2O_3$ and therefore improved its potential use as an insulating material.


*Keywords:* Sintered porous body; Chemically synthesized; Replica method in organic matrix; $Al_2O_3$; Thermal properties

## 1. Introduction

Certain porous materials have special properties and functions that cannot normally be obtained by conventional dense counterparts. Therefore, porous materials are now used in many applications such as final products and in various technological processes. Macroporous materials are used in various forms and compositions in everyday life; e.g. polymeric foams, packaging, lightweight aluminum structures in buildings, aircraft, and as a porous ceramic for water.[1,2]

A growing number of applications that require advanced ceramics have appeared in recent decades, especially in environments where high temperatures, extended wear and corrosive environments are present. Such applications include the filtration of molten metals, high temperature insulation, support for catalytic reactions,[3] filtration of particulates from exhaust gases of diesel engines and filtration of hot gases in various corrosive industrial processes, for example.[4–6] The advantages of using porous ceramic for these applications are generally a high melting point, suitable electronic properties, good corrosion resistance and wear resistance in combination with the characteristics acquired by the replacement of the solid material by voids in the component. Such characteristics include low thermal mass, low thermal conductivity, permeability control, high surface area, low density, high specific strength and a low dielectric constant.[1,7] These properties can be tailored for each specific application by controlling the composition and microstructure of the porous ceramic.[8,9]

This paper demonstrates a simple and versatile method for the preparation of porous sintered bodies obtained by the impregnation of organic fibers. Porous $Al_2O_3$ bodies have been synthesized by a mixed method of chemical synthesis[10] and replica organic matrix[1] to obtain sintered porous bodies with thermal properties suitable for applications in refractory materials.

* Corresponding author. Tel.: +55 53 3228 3705; fax: +55 53 3228 3705.
*E-mail address:* sergiocava@gmail.com (S. Cava).

0955-2219/$ – see front matter © 2012 Elsevier Ltd. All rights reserved.
http://dx.doi.org/10.1016/j.jeurceramsoc.2012.11.009

## 2. Methodology

α-$Al_2O_3$ was prepared from aluminum nitrate in an aqueous solution where organic fibers were dispersed and cotton impregnated.

For the synthesis of aluminum hydroxide, the initial aluminum nitrate – $Al(NO_3)_3{\cdot}9H_2O$ (Synth) was diluted in water. Then the solution was heated on a hot plate at 80 °C until a complete solution was obtained. Ammonium hydroxide – $NH_4OH$ (Vetec) was added until pH = 9 was reached; a ratio of $Al(NO_3)$:$NH_4OH$ 1:6 was maintained. Anhydrous citric acid – $C_6H_8O_7$ (Synth) was added until pH = 1 was reached, The ratio between $Al(NO_3)$:citric acid was 3:1 which precipitated aluminum nitrate in aluminum hydroxide, according to Eq. (1).

$$Al(NO_3)_3 + 3NH_4OH \rightarrow Al(OH)_3 + 3HN_4NO_3 \quad (1)$$

Then the process for the impregnation of aluminum hydroxide was initiated in organic fibers using the organic matrix embedding method.[1] The organic matrix was used for the cotton trade (Johnson & Johnson).

When the impregnation procedure for precursor solutions in the organic matrix was completed, the samples were placed in the electric oven (Model FE-1300 INTI) for the removal of solvents and organic fibers followed by sintering at temperatures in the range of 100–1600 °C for 2 h with a heating rate of 2 °C/min. During this process, a phase transition[11] of aluminum hydroxide in α-$Al_2O_3$ occurred.

### 2.1. Characterization

For analysis, EDX reveals the chemical composition of porous ceramics using Shimadzu EDX-720HS Model equipment.

SEM was performed on a Simadzu Model SSX-550 microscope where we evaluated the morphology and pore structure formed by the array of metal oxides.

The crystalline phase was determined by XRD using a diffractometer Shimadzu Model XRD-6000 with CuKα radiation at 40 kV and 40 mA at a scan rate of 4°/min, 10–80°, at room temperature. The average crystallite size of the porous ceramics was estimated by the Scherrer equation[12] (see Eq. (2)) where $D_{hkl}$ = the average particle diameter, $K$ = constant depending on particle shapes, $\lambda$ = the wavelength of the electromagnetic radiation, $\theta$ = the angle of diffraction and $\beta$ = the full width half maximum (FWHM).

$$D_{h\,k\,l} = \frac{K\lambda}{\beta\cos(\theta)} \quad (2)$$

The determination of the surface area of the porous bodies and the pore diameter estimated using Barret–Joyner–Halenda (BJH) method were performed on a Model AS-1 Quantachrome instrument. Adsorption and desorption isotherms were obtained with the acquisition of 40 points, and the surface area was determined using 5 reference points.

The porosity of the fibers was calculated using Eq. (3),[7] where $P$ = porosity, $\rho_{real}$ = true density and $\rho_{theoretical}$ = theoretical density.

$$P = 1 - \frac{\rho_{real}}{\rho_{theoretical}} \quad (3)$$

A TG analysis of the porous alumina body was performed in a NETZSCH TG 209 F1 thermal analyzer using 10 mg samples heated to 25–900 °C in air at a rate of 10 °C/min.

The specific heat and thermal difusidade are determined from the record of temperature rise on the opposite face of a sample of material in the form of a small disc, whose front face is subjected to an intense flash of energy supplied or by a laser or a flash lamp. Thermal conductivity is a specific characteristic of each material, and depends strongly on the temperature and the purity of the material (especially at low temperatures).

The thermophysical property determination was performed by the Laser Flash method[13–15] which facilitates the determination of the thermal diffusivity and specific heat of the sample. The power was supplied by a laser that has a maximal power output of 90 W. The energy and irradiation times are of the order of 10 ms. The measurements were made at room temperature and atmosphere.

The thermal diffusivity is calculated from the sample thickness and time required for the temperature of the opposite face achieves a given percentage of its maximum (usually time equivalent to 50% of executable rights test). The specific heat is calculated from the density (geometrically determined) and sample thickness, the maximum temperature reached on its opposite face, and the amount of heat delivered to it. The thermal conductivity is calculated by the product of the thermal diffusivity, specific heat and density, according to Eq. (4) where $K$ = thermal conductivity, $\alpha$ = thermal diffusivity, $\rho$ = density and $C_p$ = specific heat.

$$K = \alpha \cdot \rho \cdot C_p \quad (4)$$

## 3. Results

An EDX analysis showed 98.9% by weight of alumina in the porous $Al_2O_3$ body which indicates a high purity $Al_2O_3$. Fig. 1 shows the decomposition of organic fibers and aluminum hydroxide.[16] XRD patterns of samples in various temperatures suggest that phase changes occur at 200 °C, 300 °C, 400 °C, 600 °C, 700 °C, 1100 °C and 1600 °C. The material phases agree with those phases obtained using the method of a solution precursor cation embedded in fibrous cotton organic matrix under high temperatures which profit from the reactive activity of decomposition and the reaction of fibers/aluminum hydroxide appears at 600 °C but disappears at 700 °C. At 700 °C, the positions of all peaks agree with the positions of number 46-1212 of the JPCDS file (see Fig. 1) which suggests that a completely crystallized $Al_2O_3$ product was obtained. A crystalline $Al_2O_3$ is obtained by the step-wise transition of $Al(OH)_3$ + cotton fibers between 300 °C and 700 °C. The results indicate that $Al_2O_3$ is the rhombohedral space group R-3C (167). Peaks were observed relative to α-$Al_2O_3$, and its crystalline peaks are identified in the X-ray

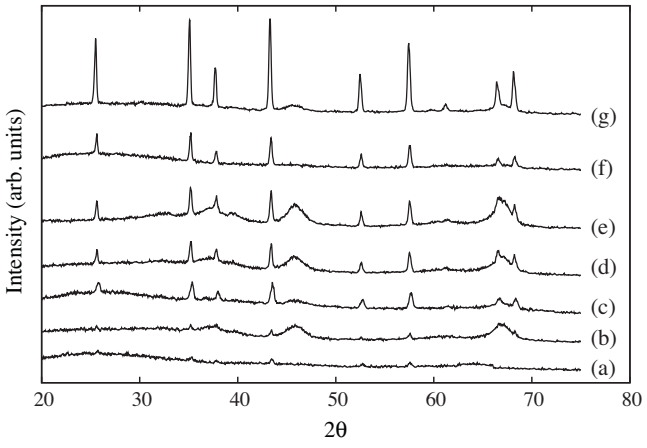


Fig. 1. X-ray diffractogram of the $Al_2O_3$ porous bodies at temperatures of (a) 200 °C, (b) 300 °C, (c) 400 °C, (d) 600 °C, (e) 700 °C, (f) 1100 °C and (g) 1600 °C.

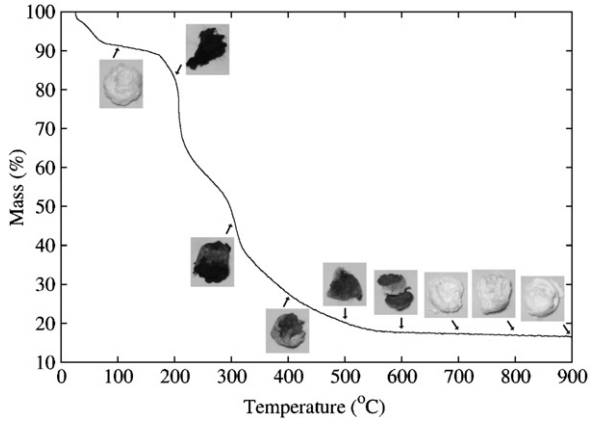


Fig. 2. Thermogravimetric analysis of the $Al_2O_3$ porous bodies.

diffractogram shown in Fig. 1 as determined by the Scherrer equation,[12] the average crystallite size is ∼350 nm at 1600 °C.

The method of embedding a cotton fiber in the organic matrix is based on the impregnation of a cellular structure with a ceramic suspension or solution precursor ceramic to produce a macroporous ceramic which has the same morphology as the original porous material (cotton) as illustrated in SEM images of Fig. 3. Many cellular structures can be used as templates to produce macroporous ceramic embedding techniques for organic matrices.

The process of manufacturing ceramic fibers using cotton as a template by employing the embedding of the organic matrix[1] can be divided into two stages: the formation of the $Al_2O_3$ fiber morphology and the removal of the cotton used as a template.

The TG illustrated in Fig. 2 shows the weight loss along with images of samples at temperatures ccurring in the formation of pore bodies at a temperature of 900 °C (their microstructure is shown in Fig. 3); a gradual weight loss of weight is evident during the process. The sample weight loss was 82.5% up to 650 °C where it terminated the decomposition of the carbonaceous mass with no significant loss of mass after the complete elimination of the carbonaceous mass.

Fig. 3 shows the morphological profile of the $Al_2O_3$ porous body with an increase of 500× where the samples are very similar. This microstructural feature is expected in all samples due to the original morphology of the organic matrix (Fig. 3).

$Al_2O_3$ fibers are formed during the calcination process. After the formation of $Al_2O_3$ fibers, cotton models are removed through the decomposition process (see Fig. 2)[17] which begins below 300 °C, and terminates close to 700 °C.

Regarding the results of SEM and TG, we can view the sample development as a function of the increasing temperature. In Fig. 3b, the porous body sintered at 100 °C has a weight loss of 9% which indicates that only evaporation solvents are used in the TG analysis. In Fig. 3c, the porous body is sintered at 200 °C with a weight loss of 8% over a primary loss of 9% which indicates the evaporation of water in the sample and the beginning of the organic material evaporation. In Fig. 3d, the porous body is sintered at 400 °C with an additional weight loss of 55% which indicates the organic matter evaporation from the cotton fiber which forms the porous body.[17] In Fig. 3e, the porous body sintered at 700 °C has a mass loss of 11% and a final weight of 83% in relation to the green body which indicates the total organic matter evaporation and the formation of the defined porous body.

Densification and grain growth are two inversely proportional properties during the sintering process. The high porosity and low densification shown in SEM images of the $Al_2O_3$ porous bodies relate to a heating rate of 2 °C/min which was used during the sintering process.[18]

Table 1 illustrates physical and geometric properties of $Al_2O_3$ porous bodies. For the surface area obtained by the BET method, $Al_2O_3$ porous bodies were 14.3 $m^2/g$ as shown in the nitrogen physisorption graph of Fig. 4. The low surface area of $Al_2O_3$ porous bodies is contrasted by high porosity appearing in SEM images because the BET method measures only the surface area of pores and not around the porous body.[19–21]

Fig. 4 has the pore distribution curve which has a high importance for the study of the porous structure, being connected to the total area of the solid and uniformity.[19,21] The distribution curve of pore size was obtained using the BJH method.

For the porosity calculation by the average of 3 samples, the $Al_2O_3$ theoretical density value was assumed to be 3940 kg $m^{-3}$; the actual density was 2336 kg $m^{-3}$. We employed Eq. (3) for theoretical and actual density values; a porosity average value of 40.71% was obtained for the $Al_2O_3$ porous. Porosity values directly influence the porous body thermal conductivity.

Table 1
Physical and geometrical properties of the $Al_2O_3$ porous bodies.

| Sample | Surface area ($m^2/g$) | Pore volume ($cm^3/g$) | Pore diameter (Å) | Porosity (%) |
|---|---|---|---|---|
| $Al_2O_3$ | 14.33 | 0.01 | 42.47 | 40.71 |

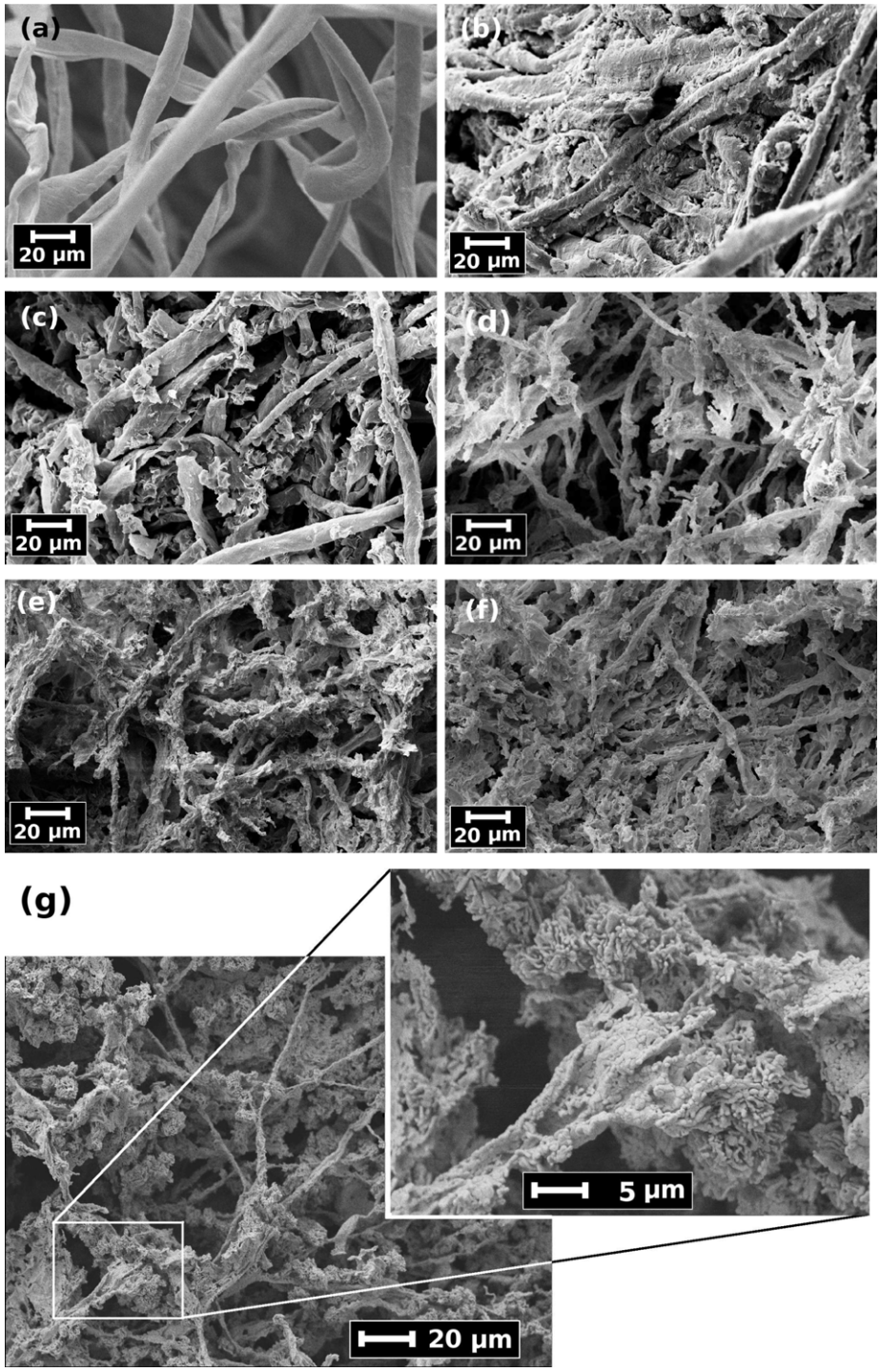


Fig. 3. SEM (a) commercial cotton and the $Al_2O_3$ porous bodies at temperatures of (b) 100 °C, (c) 200 °C, (d) 400 °C, (e) 700 °C, (f) 1000 °C and (g) 1600 °C at increased 500×.

Table 2 shows the results of thermophysical property determinations of $Al_2O_3$ porous bodies.

Some studies have been reported in the literature on the effect of porosity on reducing the thermal conductivity of solids, especially the porosity of $Al_2O_3$.[3,22] In addition to its absolute value, the grain size and porous interconnectivity and shape have a significant influence on the final thermal conductivity. Porosity-free high-purity $Al_2O_3$ with a grain size ~1 μm has a thermal conductivity of approximately 33 $W\,m^{-1}\,K^{-1}$ at room temperature[23] which is very high when compared to the results obtained for porous $Al_2O_3$ reported by Nait-Ali et al.[22] and Zivcova et al.[3] Note that for the relative thermal conductivity the grain size dependence of thermal conductivity[24,25] is irrelevant, since it is canceled out by taking the conductivity ratio.[3]

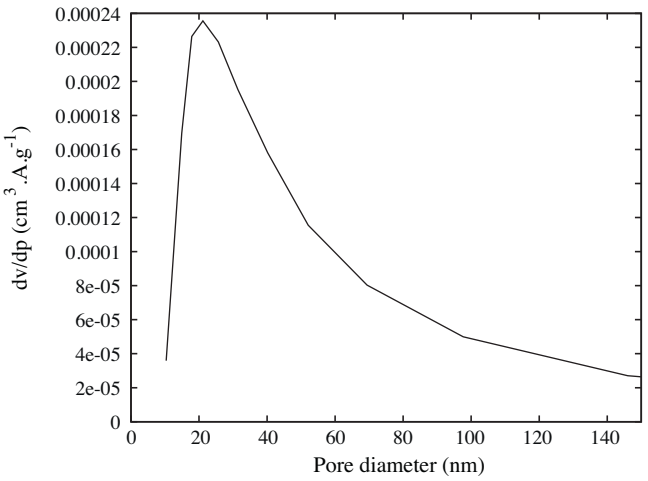


Fig. 4. Analysis of surface areas of the $Al_2O_3$ porous bodies.

Table 2
Analysis of thermal conductivity by Laser Flash method of the $Al_2O_3$ porous bodies.

| Sample | $\alpha$ ($10^6$ m$^2$ s$^{-1}$) | $\rho$ (kg m$^{-3}$) | $C_p$ (J kg$^{-1}$ K$^{-1}$) | $K$ (W m$^{-1}$ K$^{-1}$) |
|---|---|---|---|---|
| $Al_2O_3$ | 1.24 | 2336 | 561.8 | 1.63 |

Nait-Ali and co-workers, using commercial alumina and polymer as pore-forming agent, conducted a study on $Al_2O_3$ thermal conductivity with a porosity of 40% which resulted in a thermal conductivity of 9 W m$^{-1}$ K$^{-1}$ with an average grains size of 0.5 μm. Samples were sintered at 1400 °C; Zivcova and co-workers, using commercial alumina and another polymer as pore-forming agent, conducted a study on $Al_2O_3$ thermal conductivity with a porosity of 40% which resulted in a thermal conductivity of ∼5 W m$^{-1}$ K$^{-1}$ with an average grains size average of 5 μm. Samples were sintered at 1570 °C.

The obtained $Al_2O_3$ porous bodies sintered at 1600 °C have a thermal conductivity of 1.63 W m$^{-1}$ K$^{-1}$ with a porosity of 40.71% and average grain size 0.55 μm, using cotton pore-forming agent and alumina obtained by a phase transition. Correlating these values and methods with literature data shows that $Al_2O_3$ porous bodies have high refractory properties from the combination of factors such as the synthesis method, grain size and porosity, when compared to the thermal conductivity of alumina bodies analyzed at temperatures as high as 1000 °C.[26]

## 4. Conclusions

$Al_2O_3$ porous bodies composed of ceramic fibers were successfully obtained by the embedded fibrous organic matrix method with cotton as a template. SEM at different temperatures during heat treatment along with thermogravimetric analysis data indicates a step-by-step method for the complete formation of the ceramic fiber porous body. The sintering temperature, a low heating rate and the use of cotton as the organic matrix had a large effect on the surface area, the pore size and the distribution of synthesized fibers. Thermal conductivity data show excellent results when compared with the literature data due to the direct influence of the organic matrix as a template. The results show that the $Al_2O_3$ porous body is an excellent thermal insulator with direct application for refractories.

## Acknowledgements

This research was supported by the following Brazilian government funding agencies: AEB, CNPq, FINEP, FAPERGS and CAPES. We thank Ricardo Marques e Silva for obtaining SEM micrographs. Laser Flash measurements were provided by the Development Center of Nuclear Technology, Laboratory Measurement of Thermophysical Properties, Belo Horizonte, MG, Brazil.

## References

1. Studart A, Gonzenbach U, Tervoort E, Gauckler L. Processing routes to macroporous ceramics: a review. *J Am Ceram Soc* 2006;**89**(6):1771–89.
2. Ohji T, Fukushima M. Macro-porous ceramics: processing and properties. *Int Mater Rev* 2012;**57**(2):115–31, http://dx.doi.org/10.1179/1743280411Y.0000000006.
3. Zivcova Z, Gregorova E, Pabst W, Smith D, Michot A, Poulier C. Thermal conductivity of porous alumina ceramics prepared using starch as a pore-forming agent. *J Eur Ceram Soc* 2009;**29**(3):347–53.
4. Okada K, Shimizu M, Isobe T, Kameshima Y, Sakai M, Nakajima A, et al. Characteristics of microbubbles generated by porous mullite ceramics prepared by an extrusion method using organic fibers as the pore former. *J Eur Ceram Soc* 2010;**30**(6):1245–51, http://dx.doi.org/10.1016/j.jeurceramsoc.2009.11.003.
5. Okada K, Uchiyama S, Isobe T, Kameshima Y, Nakajima A, Kurata T. Capillary rise properties of porous mullite ceramics prepared by an extrusion method using organic fibers as the pore former. *J Eur Ceram Soc* 2009;**29**(12):2491–7.
6. Okada K, Imase A, Isobe T, Nakajima A. Capillary rise properties of porous geopolymers prepared by an extrusion method using polylactic acid (PLA) fibers as the pore formers. *J Eur Ceram Soc* 2011;**31**(4):461–7, http://dx.doi.org/10.1016/j.jeurceramsoc.2010.10.035.
7. Schacht C. *Refractories handbook*, vol. 178. New York: CRC; 2004.
8. Dong Q, Su H, Xu J, Zhang D, Wang R. Synthesis of biomorphic ZnO interwoven microfibers using eggshell membrane as the biotemplate. *Mater Lett* 2007;**61**(13):2714–7.
9. Dong-Dong W, Gang W, Xiao-Fei S, Ya-Ping L, Shu-Qiang D, Hong-Xia L. Fabrication of nanoporous mullite ceramics. *Chin J Inorg Chem* 2012;**28**(3):491–4.
10. Villas Bôas M, Salomão R, Pandolfelli V. Cer porosas para aplicação em altas temperaturas. *Ceramica* 2007;**53**(328):361–7.
11. Cava S, Tebcherani S, Souza I, Pianaro S, Paskocimas C, Longo E, et al. Structural characterization of phase transition of $Al_2O_3$ nanopowders obtained by polymeric precursor method. *Mater Chem Phys* 2007;**103**(2–3):394–9.
12. Cullity B, Stock S. *Elements of X-ray diffraction*, vol. 170. New York: Prentice Hall; 1972.
13. Parker W, Jenkins R, Butler C, Abbott G. Flash method of determining thermal diffusivity, heat capacity, and thermal conductivity. *Jpn J Appl Phys* 1961;**32**(9):1679–84.
14. Taylor R. Heat-pulse thermal diffusivity measurements. *High Temp–High Press* 1979;**11**(1):43–58.
15. Ferreira R, Miranda O, Dutra Neto A, Grossi P, Martins G, Reis S, et al. Implantação no cdtn de laboratório de medição de propriedades termofsicas de combustveis nucleares e materiais através do método flash laser. In: *2002 International Nuclear Atlantic Conference-INAC 2002*. 2002. p. 11–6.
16. Deng Z, Fukasawa T, Ando M, Zhang G, Ohji T. High-surface-area alumina ceramics fabricated by the decomposition of Al(OH) 3. *J Am Ceram Soc* 2001;**84**(3):485–91.

17. Fan T, Sun B, Gu J, Zhang D, Lau L. Biomorphic $Al_2O_3$ fibers synthesized using cotton as bio-templates. *Scripta Mater* 2005;**53**(8): 893–7.
18. Zhou Y, Hirao K, Yamauchi Y, Kanzaki S. Densification and grain growth in pulse electric current sintering of alumina. *J Eur Ceram Soc* 2004;**24**(12):3465–70.
19. Atkins P, Paula J. *Fsico-qumica*, vols. 1–3. Rio de Janeiro: LTC; 2004.
20. Gregg S, Sing K. *Adsorption, Surface Area and Porosity*. London: Academic Press; 1982.
21. Ciesla U, Schüth F. Ordered mesoporous materials. *Micropor Mesopor Mater* 1999;**27**(2–3):131–49.
22. Nait-Ali B, Haberko K, Vesteghem H, Absi J, Smith D. Preparation and thermal conductivity characterisation of highly porous ceramics: comparison between experimental results, analytical calculations and numerical simulations. *J Eur Ceram Soc* 2007;**27**(2–3):1345–50.
23. Pabst W, Gregorová E. Effective thermal and thermoelastic properties of alumina, zirconia and alumina–zirconia composite ceramics. *New Dev Mater Sci Res* 2007:77–137.
24. Smith D, Fayette S, Grandjean S, Martin C, Telle R, Tonnessen T. Thermal resistance of grain boundaries in alumina ceramics and refractories. *J Am Ceram Soc* 2003;**86**(1):105–11.
25. Smith D, Grandjean S, Absi J, Kadiebu S, Fayette S. Grain-boundary thermal resistance in polycrystalline oxides: alumina, tin oxide, and magnesia. *High Temperatures–High Press* 2003;**35**(1):93–100.
26. Taylor R, Dos Santos W. Effect of porosity on the thermal conductivity of alumina. *High Temp–High Press* 1993;**25**:89–98.